Available online at www.sciencedirect.com
ScienceDirect
Trans. Nonferrous Met. Soc. China 21(2011) 346−352
Transactions of Nonferrous Metals Society of China
www.tnmsc.cn

Preparation and characterization of aluminum foams with ZrH_2 as foaming agent

LI Da-wu[1, 2], LI Jie[1], LI Tao[1], SUN Ting[1], ZHANG Xiao-ming[3], YAO Guang-chun[3]

1. Department of Chemistry, College of Science, Northeastern University, Shenyang 110004, China;
2. Forensic Science & Technology Department, China Criminal Police University, Shenyang 110854, China;
3. Engineering and Researching Centre of Advanced Preparation Technology of Materials, School of Materials and Metallurgy, Northeastern University, Shenyang 110004, China

Received 26 February 2010; accepted 22 October 2010

Abstract: Aluminum foams were fabricated by melt-based route using ZrH_2 as a foaming agent. The factors which affected the foaming of aluminum foams during casting process were investigated. The powdered zirconium hydride with content of 0.6%−1.4% (mass fraction) was added to the molten pure aluminum and the foaming condition was controlled in a temperature range from 933 to 1 013 K, Ca amount of 1.5%−3.0% (mass fraction), stirring time of 0.5−2.5 min and holding time of 1.5−4.0 min to obtain homogeneous aluminum foams. The fabricated aluminum foams were characterized by XRD, SEM and Image-pro plus. The mechanical properties of the aluminum foams with different relative density were tested. The result indicates that the foaming agent (ZrH_2) is suitable for the preparation of small aperture aluminum foams with average pore diameter of 1 mm. Inter-metallic compounds and Al_2O_3 have effect on the melt viscosity. The aluminum foams experience linear elastic, platforms and densification process and had a higher efficiency of energy absorption.

Key words: aluminum foams; zirconium hydride; bubble; melt-based route

1 Introduction

Closed cell aluminum foams (CCAFs) have a good combination of properties such as high specific stiffness, high strength and good energy absorption. These characteristics make aluminum foams a potential material for absorbing impact energy during the crashing of a vehicle either against another vehicle or a pedestrian. Potential applications of these foams also exist in shipbuilding, aerospace industry and civil engineering[1]. CCAFs can be mainly produced by two methods, powder metallurgy and melt foaming[2–3]. Especially for the melt foaming method, an addition of foaming agent to the molten aluminum is useful for commercial applications because of its low cost compared with other methods. CCAF is a composite material consisting of gas and solid phases, which exhibits a porosity of 70%−90%; thus much attention is paid to the control of the morphology of the cells during foaming process. Most of the properties, such as sound absorption, heat transfer and mechanical characteristics are very sensitive to cell structure[4]. The manufacturing of CCAF includes two important considerations, firstly, the foaming agent must be able to generate a desired amount of gas bubbles with desired sizes; secondly, the molten aluminum must generate high porosity foam which is suitable for commercial use and possesses a certain viscosity so that the generated gas can be retained in the aluminum matrix during solidification.

Recently, numerous theoretical and experimental studies upon closed-cell aluminum foams have been undertaken. ZEPPELIN et al[5] investigated the decomposing behavior of foaming agent and found that various foaming agents had different foaming effects on the pore size and relative density. HAN et al[6] investigated the influencing factors on the structures of foamed aluminum using MnO_2 powder as thickening agent and TiH_2 powder as foaming agent, and sought an effective measurement to overcome the difficulties in the preparation of CCAF by melt foaming process[6]. GERGELY et al[7] studied the decomposition characteristics of $CaCO_3$ and draw a conclusion that it was well-suited to foam aluminum melts. In order to

Foundation item: Project (2004AA33G060) supported by the National High-tech Research and Development Program of China
Corresponding author: SUN Ting; Tel: +86-24-83684786; Fax: +86-24-83676883; E-mail: sun1th@163.com
DOI: 10.1016/S1003-6326(11)60720-6

improve foaming characteristics, MATIJASEVIC et al[8−9] experimentally analyzed the impact of heat treatments on TiH_2 powder, and found that the oxidation of TiH_2 particles was responsible for the observed shift in the decomposition temperature, and titanium hydride (TiH_2) and ZrH_2 can be tailored by selective oxidation and partial discharge to yield more uniform foams. ZHOU et al[10] investigated the thermal decomposition behavior of a novel gas-generating agent used for two steps foaming process of aluminum and analyzed the potential reactions between the foaming gas and the melt. YAN et al[11] investigated the preparation method and foaming mechanism of a new vesicant-mixed rare earths hydride. MONDAL et al[12] assessed experimentally the deformation response and energy absorption characteristics of closed cell aluminum-fly ash particle composite foam made by melt foaming using CaH_2 as foaming agent. Different types of blowing agents can release gas in different ways, thus cause differences in the results of foam. However, research on foaming agent of the CCAF mainly focuses on the aspects of TiH_2 because TiH_2 has strong hydrogen release and shows the best blowing agent for these alloys. However, research on aluminum by melt foaming using ZrH_2 as foaming agent was rare at home and abroad.

The preparation technology of materials and the relationship between structure and properties are the prerequisites for industrial applications of the CCAF. The work used zirconium hydride as a foaming agent to prepare more homogeneous and smaller aluminum foam. The processing parameters, such as foaming agent content, addition amount of Ca, temperature, string time and holding temperature in the melt were optimized, and their influence on the foaming properties was investigated.

2 Experimental

2.1 Materials preparation process

The CCAF was fabricated by adding foaming agent into thickened aluminum melt. The matrix material was pure aluminum (purity>99.6%), the adjuster for the control of the viscosity of the aluminum melt was pure calcium (purity>99.9%) and the foaming agent was hydride zirconium powder (purity>99%, particle size 74 μm). The CCAF was fabricated in the following steps[13]. 1) Melting: pure aluminum was melted in a crucible at 1 123 K and cooled to the desired temperature (933−1 013 K). 2) Thickening: pure calcium (1.5%−3.0%, mass fraction) was added to the melt at 1 123 K and stirred at a constant speed to make its viscosity continuously increased. 3) Mixing: when the viscosity of the melt reached a critical value, the foaming agent (0.6%−1.4%, mass fraction) was added to the melt. At the same time, the mixture was stirred at a higher speed to homogeneously disperse the powder in the whole melt. 4) Holding: the mixture in the furnace was held to decompose the foaming agent. In this stage, bubbles in the melt grew with the holding time until a cellular structure was formed. During the holding period, the structure of the melt changed obviously. The structure of the finished product was determined by evolution of bubbles in the foaming melt in this period.

2.2 Characterization

The phase and micro pore structure of foam aluminum powder were determined using XRD and SEM.

2.3 Pore structure

Valid porosity was the most important micro structural parameter of foam materials, which refers to the available volume fraction of the pores in a finished CCAF product. It could be calculated from the mass m and volume V of the sample using the previous expression[2, 13]. Pore size was another important micro structural parameter of this material. It was difficult to describe the micro structure of the CCAF by conventional methods because the distribution of the pore sizes was very wide. In this work, the size of each pore in the cross-section was determined by software analysis. The sample was dyed black using chemical staining method, and then the cross-sectional surface used for determining the pore size was polished. The pore size could be obtained using Image 5.0 after binarization image using Matlab 7.0.

2.4 Compression tests

The compression response of the CCAF using ZrH_2 as foaming agent was studied on samples with size of d 30 mm × 45 mm. Compressive specimens were loaded at a rate of 2 mm/min and measured by a CMT4000 mechanical testing machine; each test was stopped until the compression amount was above 80% of the strain.

3 Results and discussion

3.1 Effects of viscosity and content of ZrH_2 on CCAF

Thickening operation is necessary to obstruct the flotation of gas released from ZrH_2 due to rather low viscosity of molten aluminum. The influence of viscosity by changing the addition of Ca on the CCAF is indirectly examined. The results show that the valid porosity of CCAF has a very strong dependence on the viscosity of the melt. From Fig.1(a), the valid porosity continues to

decrease with the increasing content of Ca from 1.5 % to 3.0% (mass fraction), the average diameter almost linearly decreases with the addition of Ca, which suggests that Ca addition has much stronger thickening effect. The applied stirring action continues to bring air and thus continues to create additional oxides (Al_2O_3) because of thickened cell wall throughout the melt[14], resulting in much higher viscosity. At the same time, the addition of Ca may increase the amount of inter-metallic compound, for example, $CaAl_2$ and $CaAl_4$ provide more bubble nucleation medium[15−16]. The increase in viscosity reduces the surface tension of liquid metal so that the stability of bubbles can be reinforced. However, the large viscosity prevents the addition of foaming agent and obtains a high density. Therefore, the addition of Ca must be controlled between 2% and 2.5%.

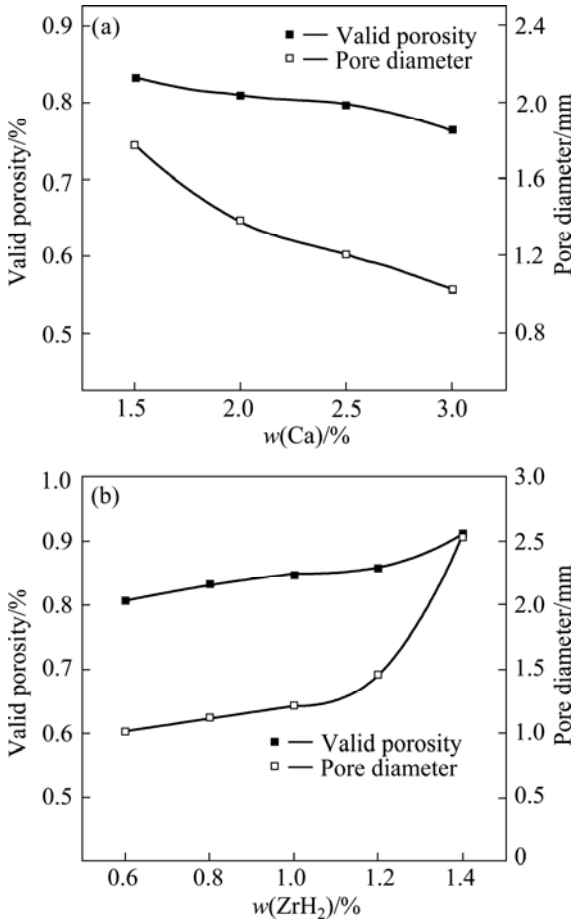

Fig.1 Effect of Ca (a) and ZrH_2 (b) contents on CCAF

Fig.1(b) shows the effects of foaming agent addition on the valid porosity and average pore diameter. The valid porosity increases with ZrH_2 addition from 0.6 % to 1.4% and the average diameter increases from 1.0 to 2.5 mm. It is evident that bubbles increase with increasing foaming agent because of more gas released from the agent, they usually merger to form a more a big hole, and yield larger pores and higher valid porosity.

Excessive addition of Ca and ZrH_2 results in unnecessarily large change in pore diameter and porosity. According to the present investigation, addition of 1.0% ZrH_2 and 2.0%−2.5% Ca is suitable for better product made of commercially pure aluminum.

3.2 Effect of temperature on foam structures

Figure 2 shows the influence of foaming temperature on the pore diameter and porosity. It is obvious that the porosity changes little when the temperature is below 700 °C, while the pore diameter increases steeply above 700 °C. Foaming temperature directly affects the melt surface tension and the foaming agent decomposition. The relationship of melt surface tension and temperature range from 660 to 710 °C is calculated as[17]:

$$\sigma = 842-0.204(T-T_m) \quad (1)$$

where σ is the surface tension of melt, T is the experimental temperature and T_m is the melt point. Surface tension is known to decrease with increasing temperature, therefore, the stability of the bubble is reduced with increasing temperature. The foaming agent may decompose gas quickly at high temperature[8] and make the experiment too difficult to control. The viscosity decreases and the stability of bubbles reduces at a certain temperature, and increases the trend of the bubble mergence and the capacity of the escaped gas, as a result, non-uniform pores can be obtained. In addition, a lot of foaming agent disappears at high temperatures during adding process. Therefore, the addition of foaming agent should be as much as possible at a relatively low temperature. According to the present investigation, the foaming process ought to be controlled between 680 and 700 °C.

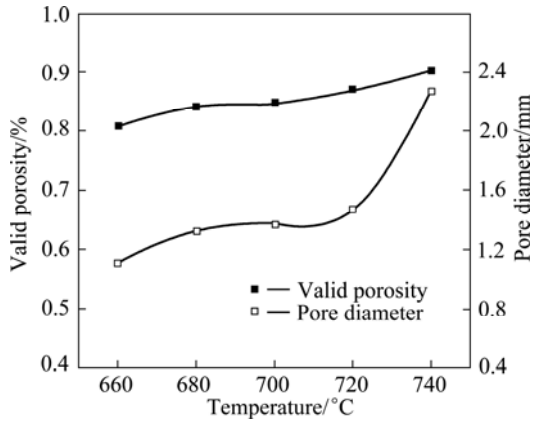

Fig.2 Effect of foaming temperature on foam structures

3.3 Effect of stirring and holding time on CCAF

Figure 3 shows the effects of stirring and holding time on the CCAF. The valid porosity continues to decrease with increasing stirring time from 0.5 to 1 min

and changes little after stirring for 1 min. The average diameter shows a similar trend with the valid porosity. However, the valid porosity increases with increasing holding time from 2.5 to 4 min. Fig.3(b) shows the effect of holding time on the CCAF. The optimal control condition occurs at stirring time of 1.5 min and holding time of 2.5 min. The stirring process aims to make the foaming agent particles disperse uniformly, so it is critical to obtain suitable stirring time. Too short or too long stirring time is not suitable to fabricate the CCAF. Holding is a process of gas growing which has effect on the pore shape[13]. In the initial period, the gas begins to grow, and the pore is circle-shaped; when the volume of gas in the melt reaches a certain proportion, the bubbles get crowded. Under the pressure inside the bubble, the melt among the bubbles turns into thin film. According to Laplace's law, the additional surface pressure of the big bubbles is relatively small, when it could not offer enough tension force to keep a big bubble in the sphere, the bubble gives way to the pressure from the melt and becomes a polyhedron, which forms the cellular structure. Based on the analysis above, a stirring time of about 1.5 min, holding time of 2.5−3 min and effective foaming time of about 1 min are appropriate.

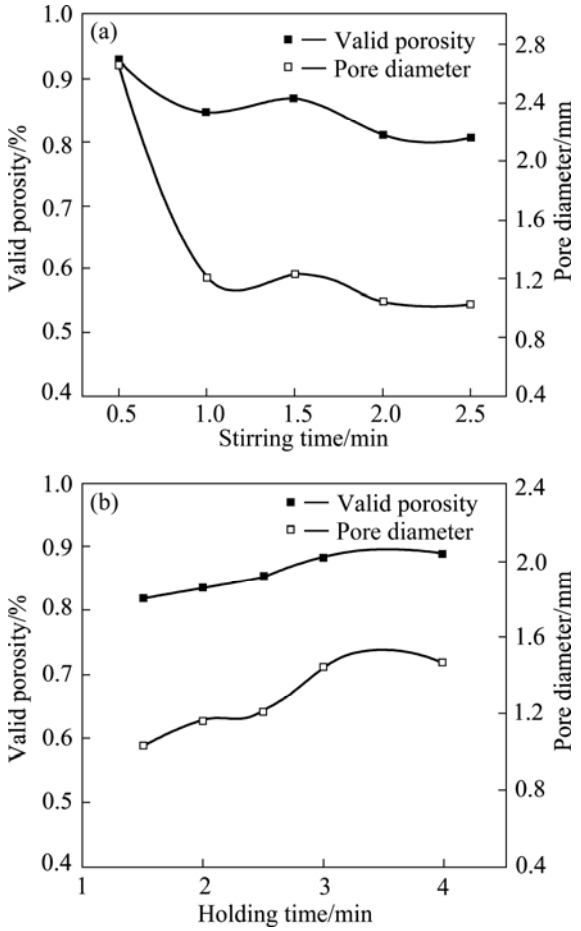

Fig.3 Effect of stirring time (a) and holding time (b) on foam structure

3.4 Characterization

It is obvious that phases play an important role in the fabrication process of CCAF. X-ray diffraction analysis was employed for the identification and quantification of the surface. Figure 4 shows that the characteristic phases in final samples are Al, Al_3Zr and Al_4Ca, while the oxides were not detected because of the low content. However, it is found in (Fig.5(a)) that there are oxides in the pores wall of matrix Al and there is Al_3Zr in inter-metallic compound in Fig.5(b). Previous studies[15−16] showed that the inter-metallic compounds had effect on the viscosity, the existence of inter-metallic compounds reduced the mobility of the melt, and the existence of $ZrAl_3$ compound could not be ignored. Due to the combined effect of three phases, Al_2O_3, Al_4Ca and Al_3Zr, a certain degree of viscosity can prevent gas bubbles mergering with each other, consequently the stability of the bubbles is reinforced.

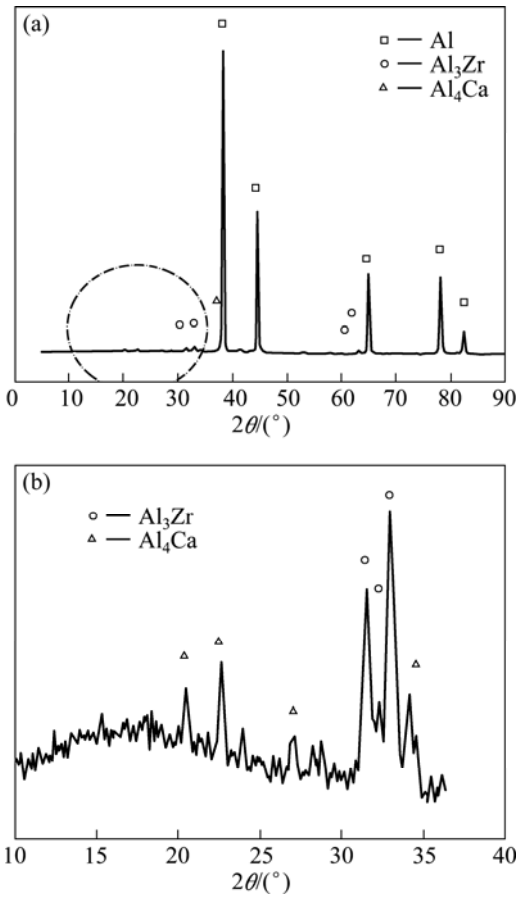

Fig.4 XRD patterns of CCAF (Fig.4(b) shows detail with enlarged scale)

In the melt, there are reactions as follows:

$$ZrH_2(s)=Zr(s)+H_2(g)$$
$$\Delta G_1/(kJ\cdot mol^{-1})=169.0-0.1347T \quad (2)$$

$$ZrH_2(s)+O_2(g)=ZrO_2(s)+H_2(g)$$
$$\Delta G_2/(kJ\cdot mol^{-1})=-931.6+0.0591T \quad (3)$$

$$2Al(l)+1.5O_2(g)=Al_2O_3(s)$$
$$\Delta G_3/(kJ\cdot mol^{-1})=-1676.49+0.3134T \quad (4)$$

$$3ZrO_2(s)+4Al(l)=3Zr(s)+2Al_2O_3(s)$$
$$\Delta G_4/(kJ\cdot mol^{-1})=-51.18+0.04544T \quad (5)$$

$$Zr(s)+3Al(l)=ZrAl_3(s)$$
$$\Delta G_5/(kJ\cdot mol^{-1})=-41.0+0.0387T \quad (6)$$

$$Ca(l)+4Al(l)=Al_4Ca(s)$$
$$\Delta G_6/(kJ\cdot mol^{-1})=-196.65+0.00293T \quad (7)$$

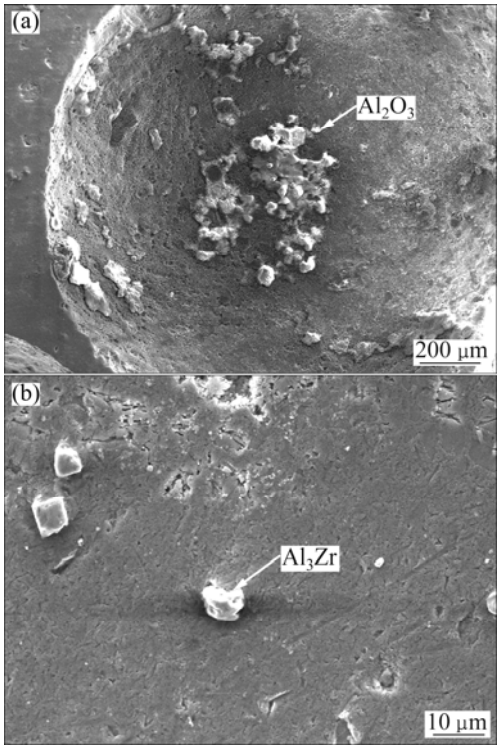

Fig.5 SEM images of CCAF

Figure 6 shows the curves of reaction free energy change (ΔG) in the range of experimental temperature. It is worth noting that although the reactions are thermodynamically favorable, they are unlikely to dominate in practice. Reaction (2) existed in steady thermodynamics state because $\Delta G_1>0$, the reaction can not occur during the process of CCAF. Reaction (3) may be considered an essential reaction because of the existence of oxygen during stirring. Reactions (4)−(7) are all thermodynamically favorable over the temperature range.

3.5 Compressive characteristics

Compression tests were performed to assess the behavior of the CCAF with different densities in a pure hydrostatic stress condition. Fig.7(a) shows the typical compression curves of the CCAF. The stress—strain curve of CCAF is smooth and shows characteristics of plastic foams which include three distinct regions, a linear elastic region, a long plateau where the stress is

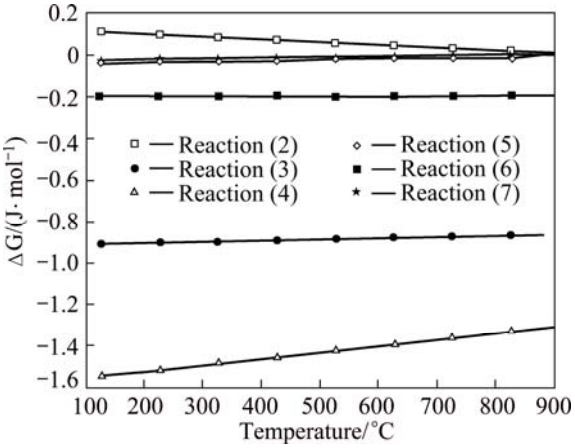

Fig.6 Curves of ΔG of reactions

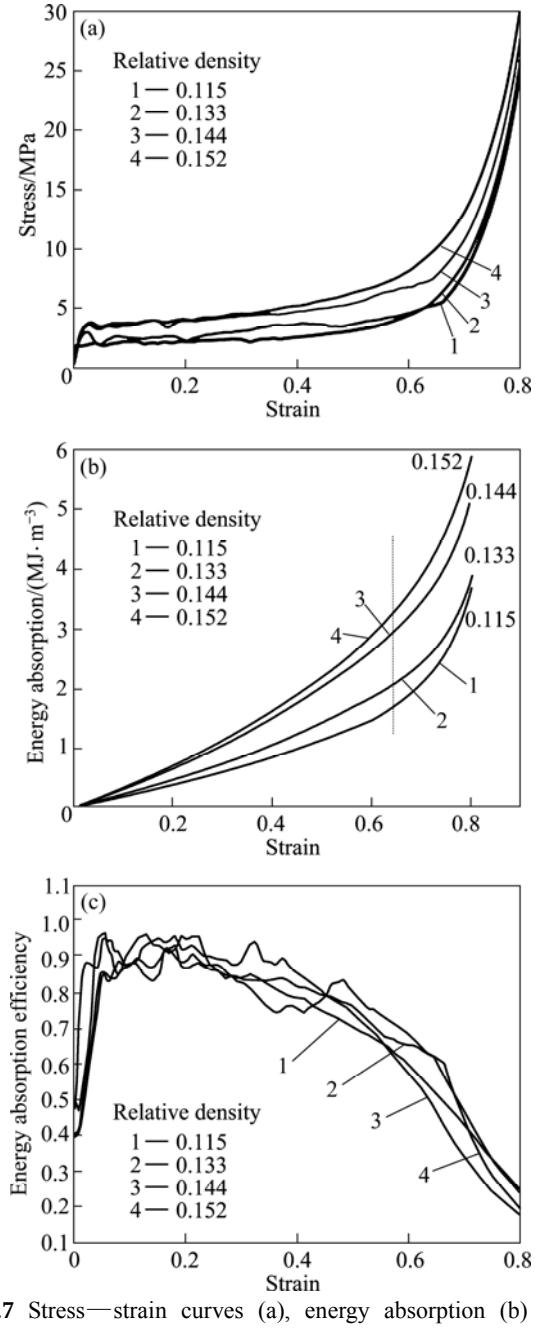

Fig.7 Stress—strain curves (a), energy absorption (b) and energy absorption efficiency (c) of CCAF with Al matrix

almost independent of strain and a final region of densification in which the stress—strain curve rises steeply.

The CCAF is mainly applied in energy absorption area, and the energy absorption capability is the energy absorbed in an unit area when the CCAF is compressed by strain. The energy absorption capability of the CCAF is calculated as[12]:

$$C = \int_0^{\varepsilon} \sigma \mathrm{d}\varepsilon \tag{8}$$

where C is the energy absorption capability and σ is the stress. Fig.7(b) shows the energy absorption capability of the CCAF calculated according to Eq.(8), which indicates that the energy absorption capability of the CCAF increases with increasing strain and shows the same trend with increasing density. The energy absorption capability of CCAF is 1.4 MJ/m^3 when the strain is 0.6 and the relative density is 0.115.

Another important parameter of energy absorption of the CCAF is energy absorption efficiency, which can be calculated as [12]:

$$\eta = \frac{\int_0^{\varepsilon} \sigma \mathrm{d}\varepsilon}{\sigma_{\max}\varepsilon} \tag{9}$$

where η is the energy absorption efficiency; σ is the stress; ε is the strain and $\sigma_{\max}$ is the maximal stress when the strain ranges from 0 to ε. The energy absorption efficiency of specimens is shown in Fig.7(c). The curves comprise three main stages: 1) Energy absorption efficiency rapidly increases with increasing strain from 0 to 0.1, and the highest value is above 90%; 2) When strain increases from 0.1 to 0.35, energy absorption efficiency shows a trend of slow rising, the curve shows an obvious fluctuation, but the energy absorption efficiency comes up to a highest value of 95%; 3) Energy absorption efficiency decreases slowly from 70% to 20% when strains increase from 0.35 to 0.8. With increasing strain in the stage, the initial collapse becomes more and more remarkable, which leads to the increasing instability to load external force, so the energy absorption capability of unit strain becomes fluctuated, resulting in the decrease and instability of energy absorption efficiency.

4 Conclusions

1) Proper control of the process parameters, such as Ca addition, ZrH_2 content, experimental temperature and stirring and holding time, leads to the production of CCAF with a uniform cell structure and high porosity. The average pore size and porosity change little with 0.6%−1.2% ZrH_2, while the average pore size and porosity increase with increasing foaming temperature and shows essentially linear relationship with Ca addition. CCAF with average pore diameter of 1.2 mm and uniform distribution was obtained under the optimum parameters of the addition of 1.0% ZrH_2 and 2.5% Ca, temperature of 680 °C and stirring time and holding time of 1.5 min and 2.5 min, respectively.

2) Intermetallic compounds and Al_2O_3 were involved in the process of increasing viscosity, and the role of compound $ZrAl_3$ could not be ignored.

3) The deformation process was mainly characterized by three stages, linear elastic sage, platform and densification stage. The energy absorption capability of CCAF increased with increasing strain and density and had a higher energy absorption efficiency of 0.95.

References

[1] EDWIN R R, DANIEL B S S. Structural and compressive property correlation of closed-cell aluminum foam [J]. Journal of Alloys and Compounds, 2009, 467(1−2): 550–556.

[2] MATIJASEVIC L B, BANHART J, FIECHTER S, GÖRKE O, WANDERKA N. Modification of titanium hydride for improved aluminum foam manufacture [J]. Acta Materialia, 2006, 54(7): 1887−1900.

[3] LI Bing, CAO Zhuo-kun, WANG Yong, YAO Guang-chun, HUA Zhong-sheng. Formation and control of bubble-free layer during preparation of Al foam by foaming in melt [J]. The Chinese Journal of Nonferrous Metals, 2008, 18(7): 1268−1273. (in Chinese)

[4] JIANG Bin, WANG Ze-jun, ZHAO Nai-qin. Effect of pore size and relative density on the mechanical properties of open cell aluminum foams [J]. Scripta Materialia, 2007, 56(26): 169−172.

[5] ZEPPELIN F V, HIRSCHER M, STANZICK H, BANHART J. Desorption of hydrogen from blowing agents used for foaming metals [J]. Composites Science and Technology, 2003, 63(16): 2293−2300.

[6] HAN Fu-sheng, WEI Jian-ning, CHENG He-fa, GAO Jun-chang. Effects of process parameters and alloy compositions on the pore structure of foamed aluminum [J]. Journal of Materials Processing Technology, 2003, 138(1−3): 505−507.

[7] GERGELY V, CURRAN D C, CLYNE T W. The foamcarp process: Foaming of aluminium MMCs by the chalk-aluminium reaction in precursors [J]. Composites Science and Technology, 2003, 63(16): 2301−2310.

[8] MATIJASEVIC L B, BANHART J. Improvement of aluminium foam technology by tailoring of blowing agent [J]. Scripta Materialia, 2006, 54(4): 503−508.

[9] MATIJASEVIC L B, GÖRKE O, SCHUBERT H, BANHART J. Zirconium hydride-a possible blowing agent for making aluminium alloy foams [C]//NAKAJIMA H, KANETAKE N. Porous Metals and Metal Foaming Technology. Japan: The Japan Institute of Metals, 2006: 107−110.

[10] ZHOU Xiang-yang, ZHANG Hua, LIU Xi-quan, LIU Hong-zhuan. Thermal decomposition behavior of novel gas-generating agent used for two steps foaming process of aluminum [J]. The Chinese Journal of Nonferrous Metals, 2008, 18(12): 2265−2269. (in Chinese)

[11] YAN Fu-xue, ZHAO Kang, GU Chen-qin. Fabrication of aluminum foams by a new vesicant-mixed rare earths hydride [J]. Journal of the Chinese Rare Earth Society, 2005, 23(2): 186−189.

[12] MONDAL D P, GOEL M D, DAS S. Compressive deformation and

energy absorption characteristics of closed cell aluminum-fly ash particle composite foam [J]. Materials Science and Engineering A, 2009, 507(1−2): 102−109.

[13] SONG Zhen-lun, ZHU Jin-song, MA Li-qun, HE De-ping. Evolution of aluminum foams structure in foaming process [J]. Materials Science and Engineering A, 2001, 298(1): 137−143.

[14] HUNTER T N, PUGH R J, FRANKS G V, JAMESON G J. The role of particles in stabilising foams and emulsions [J]. Advances in Colloid and Interface Science, 2008, 137(2): 57−81

[15] HIDETOSHI U, SHIGERU A. Effects of calcium addition on the foamability of molten aluminum [J]. Light Metal, 1987, 37(1): 42−47. (in Japanese)

[16] BABCSAN N, LEITLMEIER D, BANHART J. Metal foams—high temperature collids part Ⅰ. Ex situ analysis of metal foams [J]. Colloids and Surfaces A, 2005, 261(1−3): 123−130.

[17] BO-YOUN H, SOO-HAN P, ARAI H. Viscosity and surface tension of Al and effects of additional element [J]. Materials Science Forum, 2003, 439: 51−56.

以 ZrH_2 为发泡剂的泡沫铝制备和表征

李大武[1,2], 李 杰[1], 李 涛[1], 孙 挺[1], 张小明[3], 姚广春[3]

1. 东北大学 理学院化学系, 沈阳 110004;

2. 中国刑警学院 痕迹检验技术系，沈阳 110854;

3. 东北大学 材料与冶金学院教育部材料先进制备技术工程研究中心，沈阳 110004;

摘 要：使用氢化锆为发泡剂，通过熔体发泡法制备泡沫铝并研究其影响因素。制备工艺为：添加 0.6%−1.4%的发泡剂，1.5%−3.0%Ca(质量分数)作为增粘剂，发泡温度 933−1 013 K，搅拌时间为 0.5−2.5 min 和保温时间为 1.5−4.0 min。利用 XRD 和 SEM 对泡沫铝样品进行表征，测试其力学性能。结果表明，在合适的工艺参数下能制备出孔径均匀的泡沫铝，采用氢化锆为发泡剂可以制备出平均孔径为 1 mm 左右的泡沫铝。金属间化合物和 Al_2O_3 的存在影响熔体的粘度。泡沫铝的力学性能经历线弹性区、平台区和致密化区并表现出较高的能量吸收效率。

关键词：泡沫铝；氢化锆；气泡；熔体发泡法

(Edited by FANG Jing-hua)